Journal of Advanced Manufacturing Systems
Vol. 20 (2021) 1–17

DOI: 10.1142/S0219686721500384

Using Hybrid Artificial Neural Network and Particle Swarm Optimization Algorithm for Modeling and Optimization of Welding Process

Mohammad Mahdi Tafarroj*, Masoud Azadi Moghaddam*, Hamid Dalir† and Farhad Kolahan*,‡

*Department of Mechanical Engineering
Ferdowsi University of Mashhad, Mashhad, Iran

†Operation and Maintenance (O&M)
MAPNA Group Mashhad, Iran
‡kolahan@um.ac.ir

Published 25 May 2021

This study addresses a hybrid procedure used for modeling and optimization of gas tungsten arc (GTA) welding process of AL5052 alloy. There are different process input parameters among which welding current (I), frequency (F), welding speed (S), and gap (G) are the most important ones considered in GTA welding process. Furthermore, heat affected zone (HAZ) is considered as the most important quality measure of the process. To gather the required data for the modeling and optimization purpose, design of experiments (DOE) approach has been used. Image processing technique is used to take accurate measurements of HAZ values. In order to determine the relationship between process input variables and output measures, artificial neural networks (ANNs) have been used. Then, the trained ANNs have been used to find the optimal value of the outputs using particle swarm optimization (PSO) algorithm. Experiments have been done to verify the optimal levels of the input parameters. Verification results demonstrate that the proposed ANN-PSO procedure is quite efficient in modeling and optimization (with about 4% error) of GTA welding process.

Keywords: Gas tungsten arc (GTA) welding; artificial neural network (ANN); particle swarm optimization (PSO); heat affected zone (HAZ).

1. Introduction

Nowadays, Gas tungsten arc (GTA) welding process also known as tungsten inert gas (TIG) welding is frequently used for welding of Al–Mg alloys, based on the merits of its good surface quality.[1] In TIG welding process, to protect the molten weld pool and filler wire (if requires) from atmospheric contaminants, an inert gas like argon/helium (or combination of both) is being used. Furthermore, the electrode used for this process is a nonconsumable ones.[2] In welding processes, the quality of the

‡Corresponding author.

weldments is usually determined by such process quality measures as heat affected zone (HAZ).[2] HAZ is a crucial quality indicator of the joint that determines the metallurgical and microstructural changes of the weldments due to the heat generated during welding process. Usually, because of large grain microstructure, ductility and toughness of this area is poor. In addition, HAZ is prone to such defects as hydrogen blue brittleness, diffused crack and laminar tearing. Controlling the heat input and the subsequent HAZ could result in a proper microstructural and metallurgical properties.[3]

Various factors influence the area of HAZ created in GTA welding process. Welding current (I) and welding speed (S), frequency (F), and gap (G) are the most important variables affecting GTAW process.[2] Therefore, to achieve full penetrated weld with minimum HAZ, process parameters selection must be carefully taken into account. Conventionally, expert operators choose parameters based on time consuming trial and error method to obtain a welded joint with the required specifications. Then joint parts are examined to determine whether they meet the specifications or not.[1] The inherent nonlinearity of GTA welding process and various interactions between its input parameters have motivated the researchers to employ different modeling techniques and heuristic algorithms.[2–6] To gather experimental data needed for modeling, design of experiments (DOE) technique has been employed in many studies.[7–9]

Along this line, orthogonal array-Taguchi (O-Taguchi) technique has been used by Srirangan and Paulraj[2] to determine the experiments needed for modeling of GTAW process. The input variables chosen were the welding current, voltage, and welding speed. The output measures for quality targets chosen were the ultimate tensile strength (UTS) and yield strength. Grey relational analysis (GRA) was applied to optimize the input parameters simultaneously considering multiple output variables. Analysis of variance (ANOVA) method was used to assess the significance of factors on the overall quality of the weldments.

Conventional regression analysis has been used on some experimental data of a TIG welding process by Dutta and Pratihar.[4] Furthermore, a back propagation neural network (BPNN) and a genetic neural system (GA-NN) have been compared. Moreover, GA-NN was found to perform better than the BPNN, in most of the test cases.

The pulsed current tungsten inert gas (PCTIG) has been used by Madadi *et al.*[10] to decrease excess heat input and melting of substrate using. The experiments have been conducted based on four-factor, five-level central composite rotatable design. The quadratic order regression method has been developed to study the correlations. The developed models have been checked for their adequacy and significance by ANOVA and confirmation tests have been carried out to check the accuracy of predicted values.

An attempt has been made to study the effect of pulsed TIG welding process parameters on dilution and mechanical properties such as notch tensile strength, hardness and impact toughness in as-welded condition by Kumar and Sundarrajan.[11]

Pulsed TIG welds exhibited lower notch tensile strength and impact toughness than the parent metal due to interdendritic network microstructure features. To optimize the pulsed TIG welding process parameters of heat treatable (Al–Mg–Si) aluminum alloy and to maximize the mechanical properties of weldments, the Taguchi method has been used. An inverse relationship has been observed between the notch tensile strength and impact toughness.

The effect of activated TIG welding process parameters on the weld bead geometry of duplex stainless steel alloy 2205 is analyzed and discussed by Korra *et al.*[12] Central composite design of response surface methodology (RSM) has been used for conducting the experiments. The input process parameters (current, torch speed, and arc gap) are varied at five levels which results in 21 experimental trials. Bead-on-plate welds were made on 10-mm-thick duplex stainless steel plates. The responses (depth of penetration, area of depth of penetration, bead width, bead height, heat-affected zone width, and aspect ratio) are measured after conducting the experiments. A second-order response surface model is developed for predicting the responses for the set of given input parameters. Then, multi-objective optimization is performed to obtain the desired weld bead geometry using desirability approach.

Nowadays, numerous mathematical methods and heuristic algorithms have also been applied to find the desired process parameters settings. Meta-heuristic algorithms, such as simulated annealing (SA), particle swarm optimization (PSO), etc., have proven to be an influential skill for solving large combinatorial optimization problems such as multi objective optimization of manufacturing processes. Kolahan and Heidari[13] modeled and optimized gas metal arc welding (GMAW) process using regression modeling and SA algorithm. Various regression models have been fitted on the experimental data to develop mathematical models. The developed models have been optimized using SA algorithm. Computational results indicated that the proposed SA method could efficiently and accurately determine welding parameters so as a desired bead geometry specification was obtained. Multiple linear regression technique has been used to develop mathematical models for weld bead shape parameters of TIG welding process. Also by using the same experimental data, an attempt has been made to model the process using artificial neural network. Then, genetic algorithmic (GA) coupled with neural model has been applied to optimize the process parameters.[14] Dhas and Kumanan[15] simulated the relationships between input and output process parameters for flux cored arc welding of the mild steel plates through regression modeling technique. They embedded the developed model into a PSO algorithm to determine optimal process parameters for minimizing of bead width. A good agreement is shown by comparison of the optimized values obtained from this technique with experimental results. Azadi Moghaddam *et al.*[16] proposed an artificial neural model coupled with PSO algorithm to simulate and optimize WBG of 316L nickel based super alloys in flux cored arc welding process. The process modeling was established *via* artificial neural network and then the developed model embedded into a PSO algorithm which optimized the process parameters. The performances of the conventional regression analysis approach,

BPNN and an ANN model coupled with GA (ANN-GA) have been compared for TIG welding process. It has been shown that ANN-based approaches could yield predictions that were more adaptive in nature compared to those of the more conventional regression analysis approach. It could be due to the fact that ANN-based approaches are able to bring adaptability, which is missing in the conventional regression analysis.[17]

2. Experimental Procedure

2.1. *Material and equipment*

In this study, A DIGITIG 250 AC/DC (GAAM-Co, Iran) semi-automatic welding machine with a 250 ampere capacity and high value of pulse frequency (up to 500 Hz) has been employed to carry out the experiments. The tungsten electrode and argon with 99.7% purity as welding shield gas was used for experiments. Figure 1 shows a schematic illustration of TIG welding process.

Experiments were carried out on AL5052 alloy sheets with dimension of 100 mm × 50 mm × 2 mm. The chemical composition and mechanical properties of this alloy are reported in Table 1.[18]

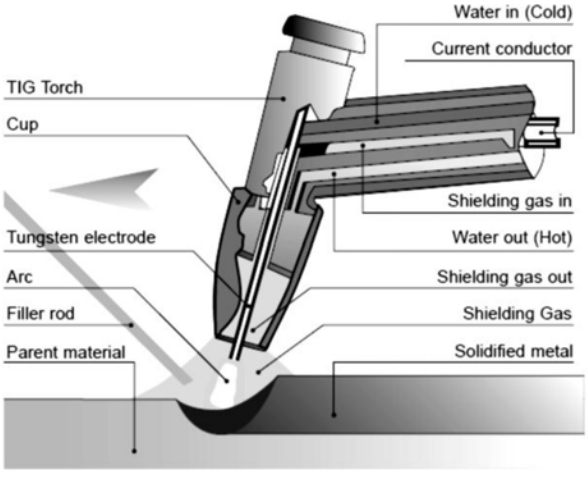

Fig. 1. A schematic representation of TIG welding process.

Table 1. Chemical composition and mechanical properties of AL5052 alloy.

Chemical composition		Mechanical properties	
Mn	2.66%	Elongation at break	30%
Fe	0.4%	Ultimate tensile strength (UTS)	193 MPa
Cr	0.19%	Modulus of elasticity	70.3 GPa
Si	0.123%	Hardness, Brinell	47 BHN
Cu	0.09%	Yield strength	89.6 MPa

AL5052 is a high-strength and nonheat-treatable Al alloy which has very good corrosion resistance to seawater and marine and industrial atmosphere. It also has very good weld ability and good cold formability. It is a medium to high strength alloy with a strength slightly higher than 5251 and a medium to high fatigue strength which is widely used in boiler making, containers, welded tubes, pressure vessels, etc.[18]

2.2. *Process input variables and their levels*

The most prominent parameters in GTA welding process include welding current (I), frequency (F), welding speed (S), and gap (G).[1–3] Likewise, HAZ has been considered as quality measure (Fig. 2). To determine the practicable working ranges of each input variable, several preliminary tests were conducted. The variable limits were then evaluated by inspecting the weldments for a smooth appearance and good penetration without any visible defects such as surface porosities and undercut. According to the preliminary test results, the input variables and their corresponding levels are listed in Table 2. Other parameters with trivial effects (electrode diameter, polarity, electrode angle, etc.) have been considered at a fixed level based on the results of preliminary tests.

2.3. *Design of experiments*

DOE approach facilitates the identification of the influence of individual parameters, establishing the relationships between process parameters and output responses, and finally determining the optimum levels of process variables in order to get the desired/optimum values of the characteristics.[19,20] According to the preliminary test results, the input variables and their corresponding levels are listed in Table 2. Other parameters with trivial effects (electrode diameter, polarity, electrode angle, etc.) have been considered at a fixed level based on the results of preliminary tests.

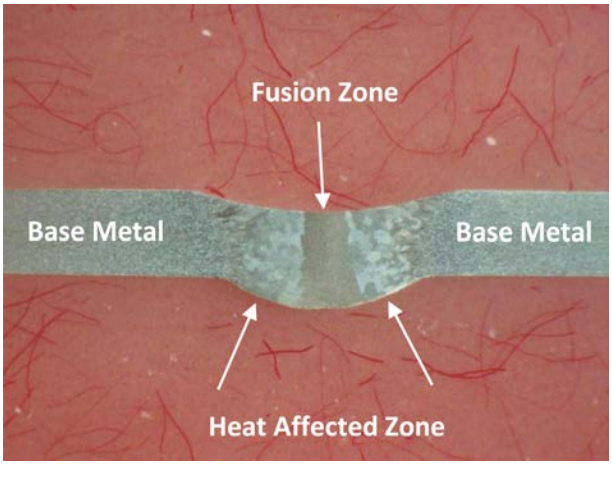

Fig. 2. Schematic illustration of heat affected zone (HAZ) area for TIG welding process.

Table 2. TIG welding process input variables and their levels.

Level	Welding speed (S)(cm/min)	Welding current (I) (Ampere)	Frequency (F) (Hz)	Gap (G) (mm)
Level 1	240	110	85	2.5
Level 2	300	120	100	3
Level 3	360	130	115	3.5

Full factorial (FF) is one of the effective techniques that can gather necessary data. Given the number of input variables and their levels, in this study FF DOE (L_{81}) has been selected to provide a well-balance design for test runs. It consists of 81 sets of process parameters, based of which the experiments have been performed. To increase accuracy, tests were carried out in random orders.[20]

After welding, three types of characteristics have been taken from each sample. For measuring HAZ, two transverse cross-sections were made on each sample. Next, the cut faces were smoothly polished and etched using 10% Nital solution to clearly show bead geometry specifications and HAZs.

Then, images were taken using an optical microscope with X10 magnification (OLYMPUS-530) (Fig. 3). These images were subsequently processed by Microstructural Image Processing (MIP) software, developed at Metallurgy Lab of Ferdowsi University of Mashhad, to determine HAZ of samples. For each sample, the average of two measurements is reported.

Figure 4 illustrates results for HAZ area using MIP software.

The GTA welding process parameters settings along with their corresponding outputs are reported in Table 3. In this table, besides the test numbers, the first four columns represent parameters settings used to perform experiments and the last column is the measured process output.

The proposed technique (hybrid ANN-PSO) is presented in Fig. 5.

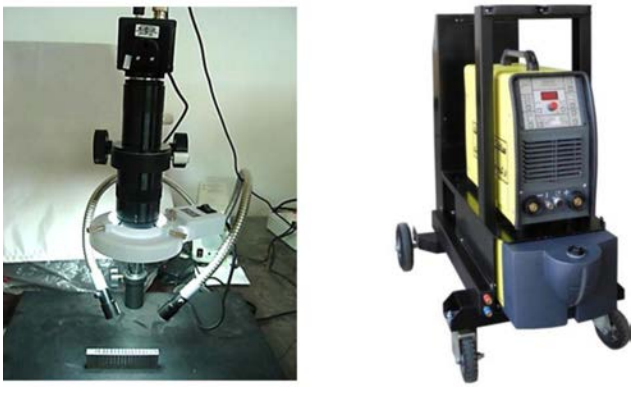

Fig. 3. Optical microscope and TIG welding machine used.

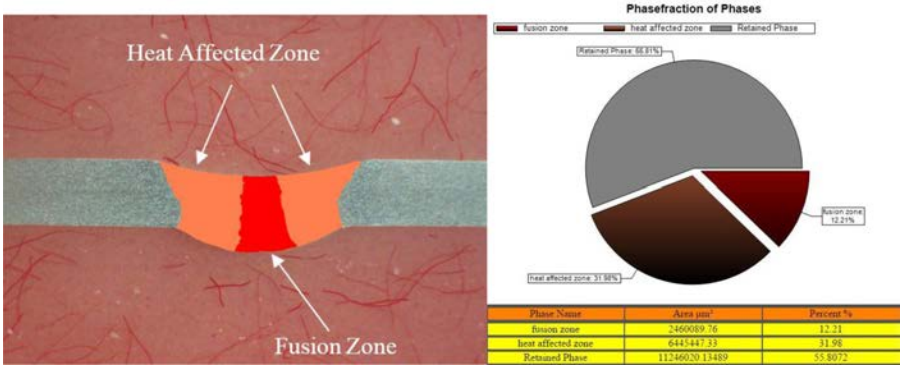

Fig. 4. Evaluation of HAZ using microstructural image processing software.

Table 3. GTA welding process experimental conditions and their corresponding results.

No.	S	I	F	G	HAZ
1	240	120	85	3.0	9.05
2	360	130	115	2.5	7.04
3	240	130	115	3.5	11.99
4	240	110	115	2.5	6.92
5	300	130	85	2.5	11.82
6	360	120	85	3.5	6.35
7	240	120	115	3.5	8.12
8	240	110	100	3.0	7.38
9	360	130	85	2.5	10.29
10	240	130	100	3.0	13.09
11	300	120	100	3.0	7.42
12	300	130	100	3.0	10.82
13	240	130	85	3.5	11.59
14	360	130	115	3.5	6.36
15	240	130	85	2.5	12.27
16	240	110	100	3.5	5.90
17	360	110	85	3.0	6.37
18	240	120	100	3.5	7.60
19	360	120	100	3.0	5.76
20	360	110	115	3.5	3.11
21	360	120	115	3.0	5.04
22	240	110	115	3.5	6.28
23	360	130	100	3.5	7.07
24	360	120	100	2.5	4.97
25	360	120	85	2.5	7.36
26	300	120	115	3.5	5.77
27	300	110	85	3.5	5.39
28	240	110	100	2.5	7.40
29	360	130	115	3.0	7.83
30	240	110	85	2.5	6.56
31	300	130	115	2.5	9.86
32	300	120	85	2.5	8.74
33	240	130	85	3.0	13.06

Table 3. (*Continued*)

No.	S	I	F	G	HAZ
34	300	110	100	2.5	6.79
35	360	110	115	3.0	4.58
36	360	110	100	3.0	6.41
37	240	120	85	2.5	8.25
38	360	130	100	3.0	8.55
39	360	130	100	2.5	7.75
40	240	130	100	2.5	12.29
41	300	110	115	2.5	5.38
42	360	110	85	3.5	4.90
43	360	110	100	2.5	4.50
44	240	120	85	3.5	9.10
45	300	130	85	3.0	11.34
46	300	110	85	2.5	6.07
47	300	110	85	3.0	6.86
48	300	110	115	3.0	6.17
49	300	110	100	3.0	7.03
50	360	120	115	2.5	4.25
51	360	120	100	3.5	5.62
52	240	120	115	2.5	8.66
53	240	130	115	2.5	12.67
54	300	120	115	2.5	6.45
55	240	120	100	3.0	9.07
56	300	130	100	3.5	9.34
57	240	130	100	3.5	11.61
58	360	110	100	3.5	3.82
59	300	130	115	3.0	10.65
60	360	130	85	3.5	8.15
61	240	130	115	3.0	13.47
62	300	120	115	3.0	7.24
63	240	120	115	3.0	9.45
64	240	110	115	3.0	7.76
65	300	120	85	3.5	6.47
66	240	110	85	3.0	8.14
67	300	120	100	2.5	6.625
68	300	130	85	3.5	9.87
69	360	120	85	3.0	6.83
70	360	110	85	2.5	5.58
71	360	130	85	3.0	10.51
72	300	110	115	3.5	3.71
73	300	120	100	3.5	5.94
74	240	110	85	3.5	5.88
75	300	110	100	3.5	4.86
76	300	120	85	3.0	9.34
77	360	110	115	2.5	3.79
78	240	120	100	2.5	4.88
79	360	120	115	3.5	6.50
80	300	130	115	3.5	10.29
81	300	130	100	2.5	10.02

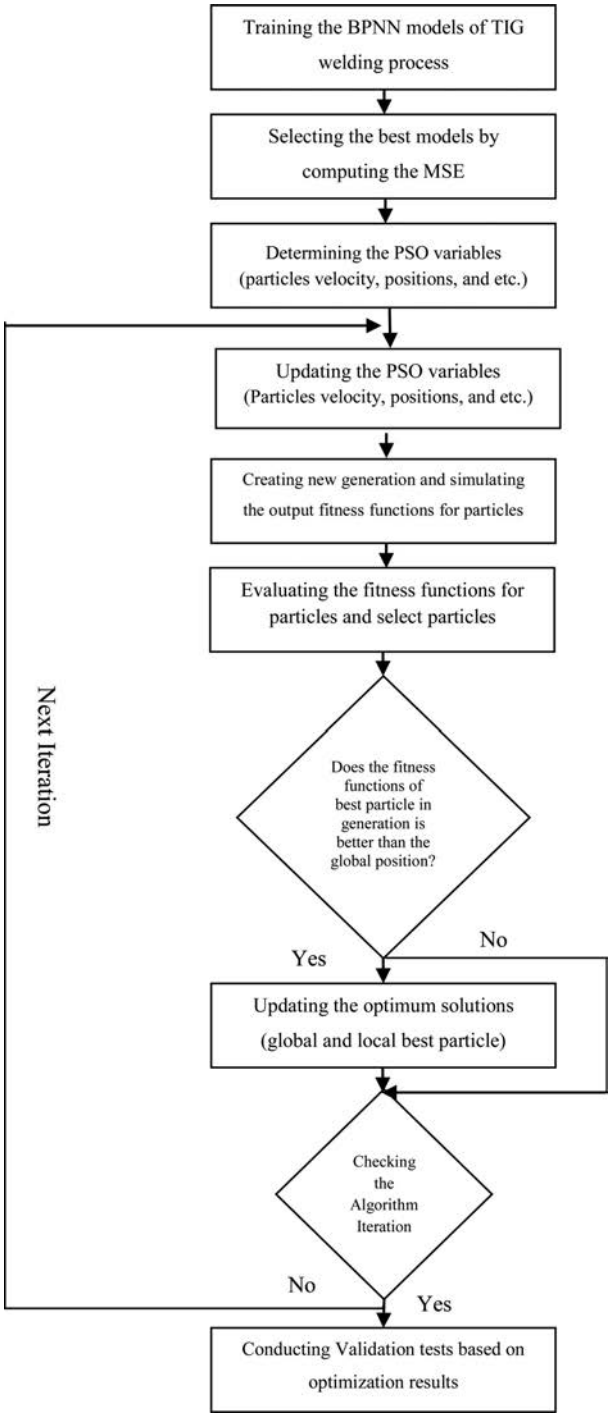

Fig. 5. Illustration of the proposed Hybrid ANN-PSO method.

3. Structure and Initialization of the Employed Back Propagation Neural Network

There are different techniques (ANFIS, regression modeling, and ANN) to relate the process input variables and output characteristics among which ANN is being extensively used based on its merits (easy programing, adaptability, and flexibility for different problems).

In this study, the ANN used is a feed forward BPNN algorithm. ANN consists of three types of layers (input layer (input variables), hidden layer, and output layer (output measures)). Implementing back propagation proceeds in three steps known as training, testing, and validation.[21] The input layer receives data from the external sources and this information has been passed to the network for processing.[22] Hidden layer, receives data from the input layer, and does all the data processing. Output layer, consisting of a linear neuron, receives processed data from the hidden layer, and sends the results out to an external receptor.[23]

In this study, data collected from the matrix of experiments consists of 81 experiments (Table 2) of which three have been excluded (experiments no. 11, 60, and 80) to assess the performance of the model used and the rest (78 experiments) has been divided into three groups (training, testing, and validating). Based on the results given in Table 4, the proposed method is quite efficient for modeling of the process.

The number of hidden layers and neurons in it has been determined through a trial and error method, in order to accommodate the converged error. In this application, two hidden layers, each with 10 neurons, have been set. There are four inputs (I, S, F, and G) and output layer consists of one neuron (HAZ) (Fig. 6). Figure 7 shows the performance of the proposed model and Fig. 8 shows the variation of mean squared error (MSE) during the training process of neural network.

4. TIG Welding Process Optimization using Particle Swarm Optimization (PSO) Algorithm

Nowadays, different heuristic algorithms for different optimization purposes have been proposed (including genetic (GA), ant colony (AC), bee colony (BC), Tabu search (TS), SA, PSO, etc.) among which PSO, based on its merits, is being extensively used. Easy programming (few input parameters to adjust) and fast convergence are the major advantages of PSO algorithm. Whereas, in high dimensional

Table 4. Outputs of the trained network for unknown inputs.

Experiment number	Process parameters				Predicted(mm)	Experiment (mm)	Relative error (%)
	I	F	S	G			
11	120	100	300	3	7.74	7.42	4.1
60	130	85	360	3.5	8.47	8.15	3.7
80	130	80	300	3.5	9.96	10.29	3.3

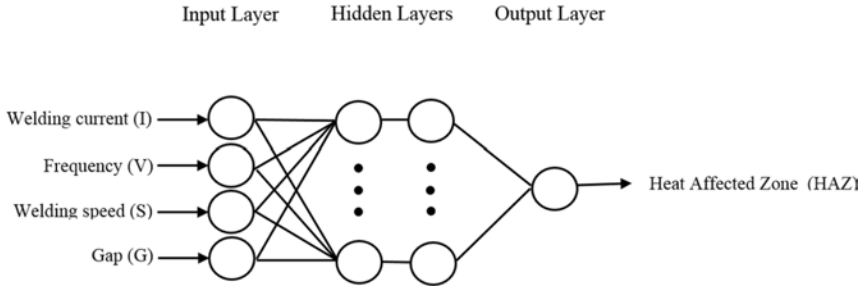

Fig. 6. Architecture of proposed artificial neural network model used.

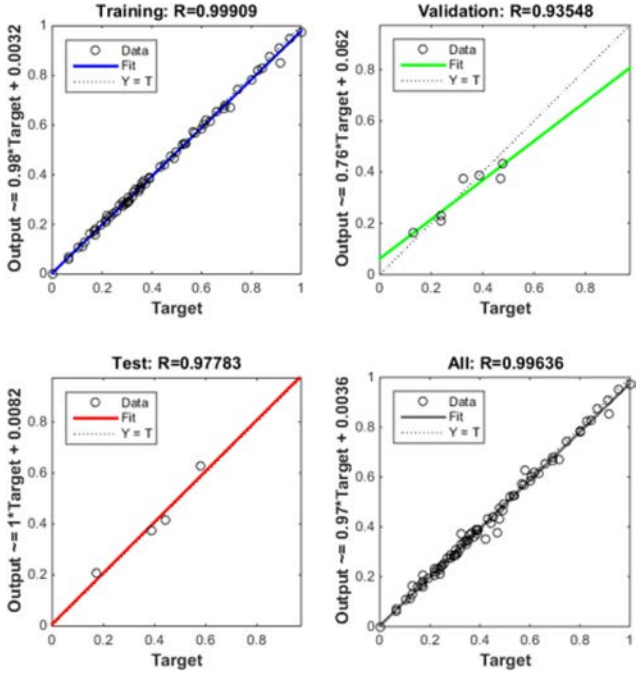

Fig. 7. Performance of the proposed model.

space, falling into local optimum traps may be considered as a weakness for PSO algorithm. GA is another extensively used algorithm for which coding is a time consuming process. A major advantage of PSO in comparison with other algorithms is its flexibility and robustness as a global search method. PSO is a very powerful and important tool in a variety of disciplines.[24] Based on the mentioned reasons above, in this study, PSO algorithm has been considered as the heuristic algorithms to optimize the welding process variables in order to minimize HAZ.

The PSO algorithm optimizes an objective function by conducting a population-based search.[25] The population consists of potential solutions, called particles. These

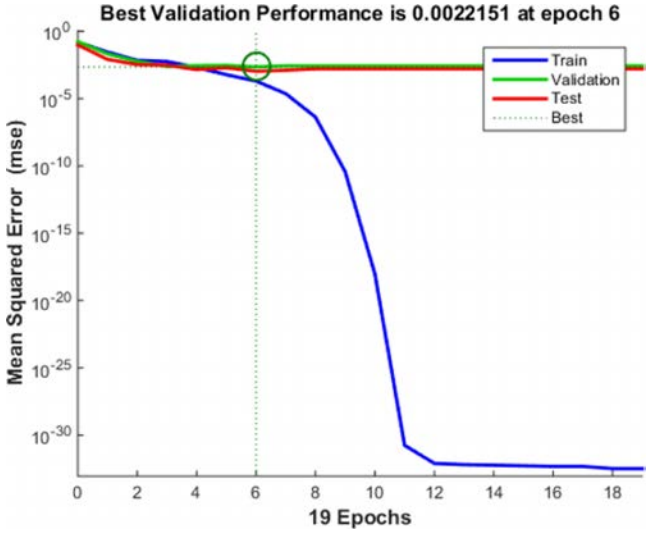

Fig. 8. Variation of mean squared error.

particles are randomly initialized and then freely fly across the multi-dimensional search space. During the flying, every particle updates its position and velocity based on the best experience of its own and the entire population. The updating policy will drive the particle swarm to move toward region with higher object value, and eventually all particles will gather around the point with highest object value. The detail of the PSO algorithm is given as follows[26,27]:

Step 1: Initialization: The velocity and position of all particles are randomly set to within pre-specified or legal range.

Step 2: Velocity updating: in each iteration the velocities of all particles are updated according to the following rule:

$$\vec{v}_i \leftarrow w \cdot \vec{v}_i + c_1 \cdot R_1 \cdot (\vec{P}_{i,\text{best}} - \vec{P}_i) + c_2 \cdot R_2 \cdot (\vec{g}_{\text{best}} - \vec{P}_i) \qquad (1)$$

where $\vec{P}_i$ and $\vec{v}_i$ are position and velocity of particle i, respectively; $\vec{P}_{i,\text{best}}$ and $\vec{g}_{\text{best}}$ are the positions with best object value found so far by particle i and the entire population, respectively; w is a parameter controlling the dynamics of flying; R_1 and R_2 are random variables from the range [0, 1]; c_1 and c_2 are factors used to control the related weighting of corresponding terms.

The inclusion of random variables endows the PSO with the ability of stochastic searching. The weighting factors, c_1 and c_2, compromise the inevitable tradeoff between exploration and exploitation.

After updating, $\vec{v}_i$ should be checked and clamped to pre-specified range to avoid violent random walking.

Step 3: Position updating: Assuming unit time interval between successive iterations, the positions of all particles are updated according to the following rule:

$$\overrightarrow{P}_i \leftarrow \overrightarrow{P}_i + \overrightarrow{v}_i \tag{2}$$

After updating, $\overrightarrow{p}_i$ would also be checked and clamped to legal range to ensure legal solutions.

Step 4: Memory updating: update $\overrightarrow{p}_{i,\text{best}}$ and $\overrightarrow{g}_{\text{best}}$ when condition is met with Eqs. (3) and (4).

$$\overrightarrow{p}_{i,\text{best}} \leftarrow \overrightarrow{p}_i \text{ if } f(\overrightarrow{p}_i) > f(\overrightarrow{p}_{i,\text{best}}). \tag{3}$$

$$\overrightarrow{g}_{\text{best}} \leftarrow \overrightarrow{p}_i \text{ if } f(\overrightarrow{p}_i) > f(\overrightarrow{g}_{\text{best}}). \tag{4}$$

where $f\left(\overrightarrow{x}\right)$ is the objective function of maximization.

Step 5: Termination checking: repeat Steps 2–4 until certain termination condition is met, such as predefined number of iterations is reached or failed to have progress for certain number of iterations. After terminating, PSO reports the $\overrightarrow{g}_{\text{best}}$ and $f\left(\overrightarrow{g}_{\text{best}}\right)_{best}$ as its solution.

The upper and lower bounds of each variable which is used in the optimization procedure are shown in Table 2. The number of particles was set to 80 and the optimization algorithm stopped when the particles are not able to improve their position or in other words, the best solutions found are not improved after 50 iterations.

Figures 9 and 10 show the variation of the best position which has been found by each individual in each iteration and the current iteration, respectively.

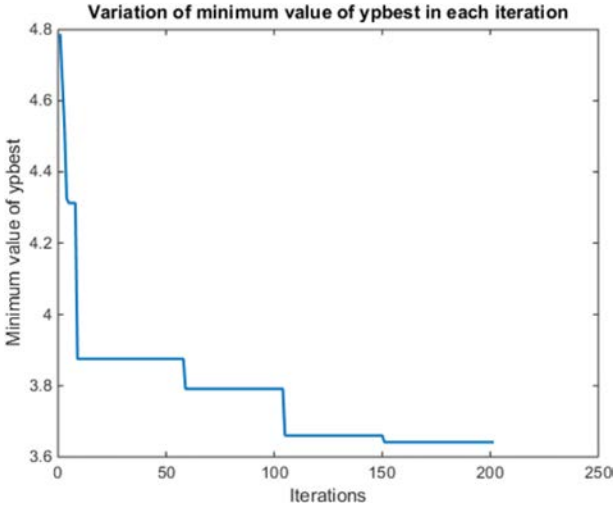

Fig. 9. Variation of the best position in each iteration.

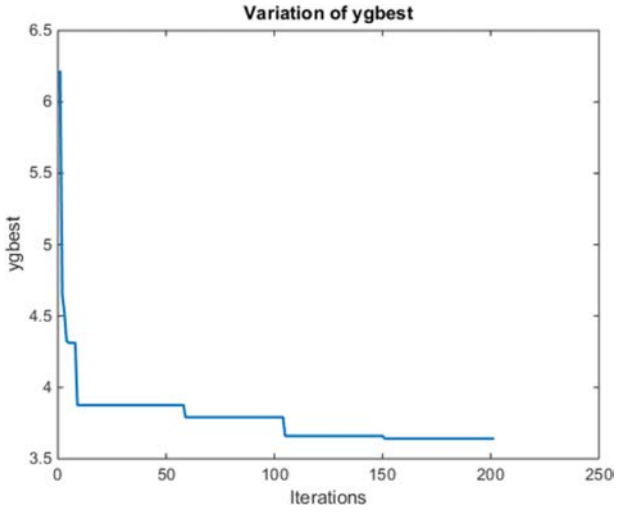

Fig. 10. Variation of the best position found by particles up to current iteration.

Table 5. Result of process optimization.

Output	Process parameters				Predicted (mm)	Experiment (mm)	Relative error (%)
	I	F	S	G			
HAZ	111	112.83	360	3.49	3.64	3.76	3
HAZ	111	112.84	360	3.49	3.64	3.81	4
HAZ	111	112.84	360	3.49	3.64	3.79	4

The optimized parameters values listed in Table 5 (the optimized experiment has been repeated three times) indicate that welding current should be roughly at its lower permissible range and others should be approximately set at highest levels, resulting in minimum possible HAZ. Evaluation of the optimized condition is shown in Fig. 11.

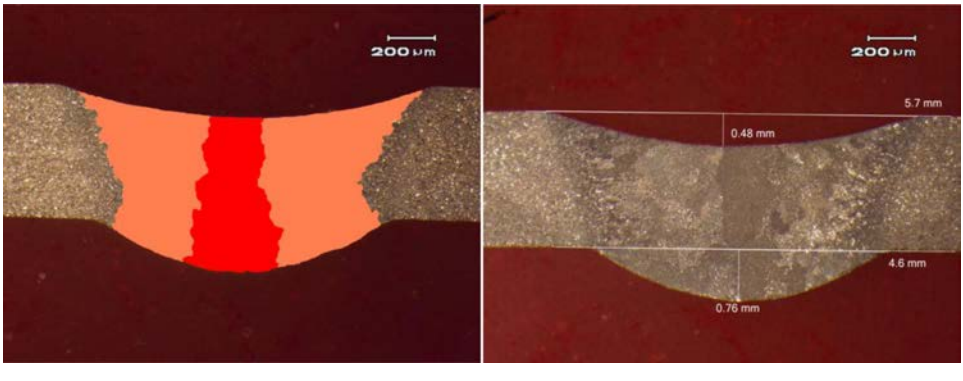

Fig. 11. Evaluation of HAZ for the optimized conditions.

5. Conclusion and Discussion

There is an extensive body of research considering modeling and optimization of different welding processes. However, to the best of our knowledge, there is no study in which HAZ has been considered, modeled and optimized using DOE, artificial neural network, and evolutionary algorithms like PSO. Therefore, this study presents a new approach based on DOE, artificial neural networks (ANNs), and PSO algorithm to establish the relations between process inputs and outputs parameters of TIG welding process and optimize them in order to minimize HAZ.

In this research, modeling and optimization of HAZ in GTA welding process for AL5052 has been addressed and the main conclusions can be summarized as follows:

- GTA welding process has been modeled using experimental data gathered by L_{81}FF design matrix.
- HAZ has been measured using MIP software.
- BPNN model has been taken into account to model and predict HAZ area.
- BPNN model has been coupled with PSO algorithm to determine the optimal set of process settings.
- The optimized parameter values, given by hybrid ANN-PSO, indicate that welding current should be set at its lower ends (111 ampere) and others approximately at their highest ends. Such settings, along with the values for other three parameters, would also produce HAZ to its minimal value.

Based on the obtained results, welding current should be set at the lowest level (111 A), frequency at the highest level (113 Hz), welding speed at the highest level (360 cm/min), Gap at the highest level (3.5 mm), to minimize the heat input and consequently the HAZ area.

For future studies in this regard, performance of different methods for modeling (regression modeling, ANFIS, ANN, etc.,) and optimization (heuristic algorithms) purposes could be considered and compared.

Compliance with ethical standards Conflict of interest

The authors declare that they have no conflict of interest.

Funding

This study was not funded.

References

1. A. V. Santhana, P. K. Babu, P. Giridharan, S. Ramesh Narayanan and V. S. Narayana Murty, Prediction of bead geometry for flux bounded TIG welding of AA 2219-T87 aluminum alloy, *J. Adv. Manuf. Syst.* **15**(2) (2016) 69–84.
2. A. Kumar and S. S. Paulraj, Multi-response optimization of process parameters for TIG welding of Incoloy 800HT by Taguchi grey relational analysis, *Eng. Sci. Technol. Int. J.* **25**(3) (2015) 112–122.

3. T. V. Cunha, A. L. Voigt and C. E. Bohórquez, Comparison of microstructure and mechanical properties of TIG and laser welding joints of a new Al–Zn–Mg–Cu alloy, *J. Mater. Process. Technol.* **231**(1) (2016) 449–455.
4. P. Dutta and D. K. Pratihar, Modeling of TIG welding process using conventional regression analysis and neural network-based approaches, *J. Mater. Process. Technol.* **184**(3) (2007) 56–68.
5. E. Ahmadi and A. R. Ebrahimi, Welding of 316L austenitic stainless steel with activated tungsten inert gas process, *JMEPEG* **24**(4) (2015) 1065–1071.
6. A. V. Santhana Babu, P. K. Giridharan, P. Ramesh Narayanan, S. V. S. Narayana Murty and V. M. J. Sharma, Experimental investigations on tensile strength of flux bounded TIG welds of AA2219-T87 aluminum alloy, *J. Adv. Manuf. Syst.* **13**(2) (2014) 103–112.
7. L. Tian, Y. Luo, Y. Wang and X. Wu, Prediction of transverse and angular distortions of gas tungsten arc bead-on-plate welding using artificial neural network, *Mater. Des.* **54**(2) (2014) 458–472.
8. R. Pamnani, M. Vasudevan, P. Vasantharaja and T. Jayakumar, Optimization of A-GTAW welding parameters for naval steel (DMR 249 A) by design of experiments approach, in *Proc. IMechE Part L: J Materials: Design and Applications* (2015), pp. 1–12.
9. R. Malviya and D. K. Pratihar, Tuning of neural networks using particle swarm optimization to model MIG welding process, *Swarm Evol. Comput.*, **1**(1) (2011) 223–235.
10. Madadi, F. Ashrafizadeh and M. Shamanian, Optimization of pulsed TIG cladding process of stellite alloy on carbon steel using RSM, *J. Alloys Compound.* **510**(1) (2012) 71–77(2012).
11. A. Kumar and S. Sundarrajan, Effect of welding parameters on mechanical properties and optimization of pulsed TIG welding of Al-Mg-Si alloy, *Int. J. Adv. Manuf. Technol.* **42**(1) (2009) 118–125.
12. N. N. Korra, M. Vasudevan and K. R. Balasubramanian, Multi-objective optimization of activated tungsten inert gas welding of duplex stainless steel using response surface methodology, *Int. J. Adv. Manuf. Technol.* **25**(4) (2005) 112–118.
13. F. Kolahan and M. Heidari, New approach for predicting and optimizing weld bead geometry in GMAW, *Int. J. Mech. Syst. Sci. Eng.* **2**(1) (2010) 138–142.
14. D. S. Nagesh and G. L. Datta, Genetic algorithm for optimization of welding variables for height to width ratio and application of ANN for prediction of bead geometry for TIG welding process, *Appl. Soft Comput.* **10**(2), (2010) 897–907.
15. J. E. R. Dhas and S. Kumanan, Optimization of parameters of submerged arc weld using non-conventional techniques, *Appl. Soft Comput.* **11**(2) (2011) 5198–5204.
16. M. Azadi Moghaddam, R. Golmezergi and F. Kolahan, Multi-variable measurements and optimization of GMAW parameters for API-X42 steel alloy using a hybrid BPNN–PSO approach, *Measurement* **92**(6) (2016) 279–287.
17. P. Dutta and D. K. Pratihar, Modeling of TIG welding process using conventional regression analysis and neural network-based approaches, *J. Mater. Process. Technol.* **184**(2) (2007) 56–68.
18. R. Ghelichi, D. MacDonald, S. Bagherifard, H. Jahed, M. Guagliano and B. Jodoin, Microstructure and fatigue behavior of cold spray coated Al5052, *Acta Mater.* **60**(2) (2012) 6555–6561.
19. M. N. Islam and A. Pramanik, Comparison of design of experiments via traditional and taguchi method, *J. Adv. Manuf. Syst.* **15**(3) (2016) 151–160.
20. B. Senthilkumar and T. Kannan, Effect of flux cored arc welding process parameters on bead geometry in super duplex stainless steel claddings, *Measurement* **62**(2) (2015) 127–136.

21. M. Manohar, T. Selvaraj, D. Sivakumar and M. George, Modeling of turning parameters for Inconel 718 alloy using ANN, *J. Adv. Manuf. Syst.* **14**(4) (2015) 203–213.
22. M. A. Ayubi Rad and M. S. Ayubi Rad, Comparison of artificial neural network and coupled simulated annealing based least square support vector regression models for prediction of compressive strength of high-performance concrete, *Sci. Iran. A* **24**(2) (2017) 487–496.
23. S. Panda and S. N. Panda, Modeling and optimization of rolling process: A multi-objective approach, *J. Adv. Manuf. Syst.* **19**(2) (2020) 343–364.
24. E. Ficarella, L. Lamberti and S. O. Degertekin, Comparison of three novel hybrid met heuristic algorithms for structural optimization problems, *Comput. Struct.* **244**(2) (2021) 145–158.
25. K. Zhi, W. Jia, G. Zhang and L. Wang, Normal parameter reduction in soft set based particle swarm optimization algorithm, *Appl. Math. Model.* **39**(3) (2015) 4808–4820.
26. K. Vipin Gopan, L. Dev Wins, G. Evangeline and A. Surendran, Experimental investigation for the multi-objective optimization of machining parameters on AISI D2 steel using particle swarm optimization coupled with artificial neural network, *J. Adv. Manuf. Syst.* **19**(3) (2020) 589–606.
27. M. M. Hasheminejad, N. Sohankar and A. Hajiannia, Predicting the collapsibility potential of unsaturated soils using adaptive neural fuzzy inference system and particle swarm optimization, *Sci. Iran. A* **25**(6) (2018) 2980–2996.